Research Article Vol. 59, No. 13 / 1 May 2020 / Applied Optics D111

applied optics

Measurement method of optical properties of *ex vivo* biological tissues of rats in the near-infrared range

Ana Sanchez-Cano,[1,2] José Eduardo Saldaña-Díaz,[3] Lorena Perdices,[2,4] Isabel Pinilla,[2,5,6] Francisco Javier Salgado-Remacha,[1,*] and Sebastián Jarabo[1]

[1]Departamento de Física Aplicada, Universidad de Zaragoza, Pedro Cerbuna 12, E-50.009, Zaragoza, Spain
[2]Instituto de Investigación Sanitaria Aragón (IIS Aragón). San Juan Bosco 13, E-50009, Zaragoza, Spain
[3]Departamento Académico de Ciencias Básicas, Universidad Nacional de Huancavelica, Facultad de Ciencias e Ingeniería, Huancavelica, Peru
[4]Instituto Aragonés de Ciencias de la Salud (IACS), San Juan Bosco 13, E-50009, Zaragoza, Spain
[5]Departamento de Cirugía, Ginecología y Obstetricia, Universidad de Zaragoza, Pedro Cerbuna 12, E-50009, Zaragoza, Spain
[6]Hospital Clínico Universitario Lozano Blesa, Oftalmología, San Juan Bosco 15, E-50009, Zaragoza, Spain
*Corresponding author: fjsalgado@unizar.es

Received 28 November 2019; revised 6 February 2020; accepted 6 February 2020; posted 6 February 2020 (Doc. ID 384614); published 12 March 2020

An optical fiber-based supercontinuum setup and a custom-made spectrophotometer that can measure spectra from 1100 to 2300 nm, are used to describe attenuation properties from different *ex vivo* rat tissues. Our method is able to differentiate between scattering and absorption coefficients in biological tissues. Theoretical assumptions combined with experimental measurements demonstrate that, in this infrared range, tissue attenuation and absorption can be accurately measured, and scattering can be described as the difference between both magnitudes. Attenuation, absorption, and scattering spectral coefficients of heart, brain, spleen, retina, and kidney are given by applying these theoretical and experimental methods. Light through these tissues is affected by high scattering, resulting in multiple absorption events, and longer wavelengths should be used to obtain lower attenuation values. It can be observed that the absorption coefficient has a similar behavior in the samples under study, with two main zones of absorption due to the water absorption bands at 1450 and 1950 nm, and with different absolute absorption values depending on the constituents of each tissue. The scattering coefficient can be determined, showing slight differences between retina and brain samples, and among heart, spleen and kidney tissues.

https://doi.org/10.1364/AO.384614

1. INTRODUCTION

The knowledge of light's behavior, both theoretical and experimental, and through many biological materials, has been widely studied to develop new noninvasive biomedical applications [1–6]. Some phenomena related to matter–light interaction, such as absorption or scattering, suppose a limit in the imaging depth capability. For this reason, it is important to reduce these losses to increase the intensity of transmitted light and achieve meaningful information at deeper penetration depths. In this sense, the forward transmitted light through turbid media consists of a combination of collimated and diffused radiation. The ballistic light is the light propagating only in the forward direction. It is considered to be a fraction of the incident light that is not affected by scattering events within the medium, retaining the characteristics of the incident beam. The attenuation of this ballistic photon intensity in a turbid medium can be estimated in terms of absorption and scattering. The multiple-scattered light emerges with in a wide range of directions after traveling long distances, whereas the slightly scattered light travels in a wriggly motion in the forward direction. The information about these optical properties allows the prediction of the limits of the measurement techniques. It has been said that infrared (IR) light penetrates deeply in tissue since the attenuation is mainly due to scattering rather than absorption. Due to the relative low absorption (around 1100–1350 nm, 1600–1870 nm and 2100–2300 nm), these spectral regions are usually called "therapeutic windows II, III, and IV," respectively [7–14].

A variety of methods can be used to completely characterize the light transmittance process through biological tissues (human or animal), based on conventional spectrophotometric systems [12,15]. An absorption coefficient can be easily obtained upon the attenuation parameters calculated from experimental transmittance spectra, using a theoretical model

for the scattering description [4,6,12,15,16]. However, there exists a high variability among spectra of any kind of tissue, due to the time of measurement, the water content (with absorption bands at 1450 and 1930 nm), the fixation procedure, and the composition of the tissue (absorption bands around 1200 nm for lipids, or 1450 nm for O-H groups) [10]. Propagation of the light and spectral features of the samples are associated with their density, structure, size and shape of the sample, content, time delay before post-mortem measurements, refractive index, their thickness, or the way the samples have been excised [10]. Recently, supercontinuum sources have been used to quantify transmission spectra in the IR range through several *ex vivo* rat tissues. Thus, it has been described that the spectral attenuation in the spleen, kidney, heart, retina, and brain fell off quickly for longer wavelengths [17,18], suggesting that similar behavior can be found in any kind of biological tissues, even blood [6], which results in a lower attenuation for longer wavelengths. The optical properties of tissue have a strong dependence on wavelength, and it is necessary to choose the proper wavelength to achieve a large penetration depth. The penetration depth is basically limited by the attenuation of ballistic light propagation (scattering and absorption), as it was previously described by OCT sources [4,19], multiphoton microscopy [20], and spectrophotometry [10,12,16].

Any improvement of image techniques over biological tissues would need an accurate measurement of the absorption and scattering coefficients. However, they cannot be accurately determined by considering only experimental measurements with the standard procedures. A retrieval procedure is necessary based usually on the radiation transfer theory (by means of the discrete ordinate method or the modified differential approximation) to solve the inverse problem [21–23]. In this paper we provide a reasonable estimation of absorption and scattering coefficients in the range between 1100 nm up to 2300 nm, based exclusively on experimental measurements. To the best of our knowledge, this study is the first one able to evaluate these coefficients with biological tissues combining these techniques in this IR spectral region.

2. MATERIAL AND METHODS

A. Experiments

Animal procedures were performed in accordance with the Statement for the Use of Animals in Ophthalmic and Vision Research by The Association for Research in Vision and Ophthalmology, Inc. (ARVO), and with the authorization and supervision of the Institutional Animal Care and Use Committee from the University of Zaragoza in Spain. Two six-month-old Sprague Dawley normal rats were anesthetized and sacrificed by administering a lethal dose of pentobarbital. The tissues were removed, fixed in 4% paraformaldehyde for 1 h at room temperature, washed in a phosphate buffer and sequentially cryoprotected in 15% sucrose for 1 h and 30% sucrose overnight at 4°C. The brain (white matter), retina, spleen, heart, and kidney tissues were sliced at different thicknesses (from 15 to 100 μm) using a cryostat (Leica Biosystems Nussloch GmbH, Nussloch, Germany) and mounted on microscope glass slides.

Two different setups were used in this work, as shown in Fig. 1. A custom-made IR spectrophotometer was used to measure the direct transmittance from 1100 to 2300 nm. The setup consisted of a broadband halogen light source chopped to 270 Hz, a monochromator Digikröm CM110 (Spectral Products, Putnam, CT, USA), an optic fiber with an output that was collimated with a 3 mm diameter beam impinging on the tissue slice, and finally an GaAs detector to measure the transmitted light. We used a custom-written Visual Basic program (National Instruments, Texas, USA) to communicate with the spectrophotometer. The installation was calibrated with a certified holmium standard (Hellma GmbH&Co.KG, Müllheim, Germany), and with NDQ neutral density filters, with 0.50 and 0.30 optical densities (CVI Laser Optics, NM, USA) to calibrate wavelength and transmittance measurements, respectively. Reference spectra were taken with a thin quartz slide, without tissue, that was placed on a sample holder.

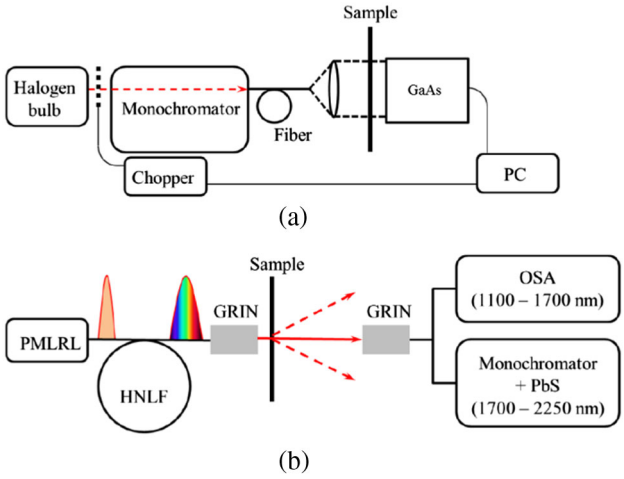

Fig. 1. (a) IR spectrophotometer and (b) supercontinuum system used in this work. PC, personal computer; PMLRL, passive mode-locked ring laser; HNLF, highly nonlinear fiber; GRIN, gradient-index lens; OSA, optical spectrum analyzer.

The supercontinuum source [Fig. 1(b)] was the same as those of Saldaña *et al.* [18]. A passive mode-locked ring laser (PMLRL) produced a train of femtosecond pulses, which were used as a seed for a highly nonlinear fiber (HNLF) to obtain a supercontinuum spectrum. The output was collimated using a gradient-index (GRIN) lens, passing through the sample and collected again with a second GRIN lens. The spectral measurements from 1100 to 2250 nm were obtained using an optical spectrum analyzer (OSA) and a monochromator with a PbS photodetector.

B. Theory

The transmittance of different tissues was measured by means of the previously described single-mode fiber collimator based on a graded-index lens [18]. Since the acceptance angle of the gradient-index lens is very small (0.15 deg.), only straightforward light is coupled into the second fiber, eliminating almost all the diffuse light. (Note: It has been experimentally verified that only a 0.1% of diffuse light is coupled). Therefore, as only the ballistic photons reach the photodetector, this method allows measurement of the spectral attenuation coefficient (due to both scattering and absorption) in agreement with the expression,

$$T_t(\lambda) = \exp[-\alpha(\lambda)L], \quad \alpha(\lambda) = \alpha_a(\lambda) + \alpha_s(\lambda), \tag{1}$$

where α is the attenuation coefficient, α_a is the absorption coefficient, α_s is the scattering coefficient, T_t is the transmission factor, L is the tissue thickness, and λ is the wavelength.

However, the transmittance of biological tissues is usually measured using a spectrophotometer [12,24,25]. Then, the transmitted power does not obey Eq. (1), and its behavior should be expressed as

$$\hat{T}_t(\lambda) = \exp[-\hat{\alpha}(\lambda)L], \hat{\alpha}(\lambda) = \widehat{\alpha_a}(\lambda) + \widehat{\alpha_s}(\lambda)$$
$$= k_a\alpha_a(\lambda) + k_s\alpha_s(\lambda), \tag{2}$$

where the coefficients k_a and k_s are included to consider an effective absorption coefficient, $\widehat{\alpha_a}$, and an effective scattering coefficient, $\widehat{\alpha_s}$. Due to multiple scattering along the tissue, the scattered photons describe a random trajectory and, consequently, the actual optical path is longer than the tissue length. Consequently, they suffer more absorption than the ballistic photons [26–28] and have an effective coefficient higher than α_a, which results in a value of k_a bigger than 1. The k_a value depends on the kind of tissue and even changes with the tissue sample [27]. Distribution of temporal delays for diffuse light has been measured in breast samples by means of a pulsed laser [26,27]. As delay values are equivalent to k_a values, it is possible to determine the average value of k_a for these samples, obtaining values of $k_a = 1.4$ [26] and $k_a = 2.5$ [27], which can be taken as reference values. We estimate that, in general, it does not seem appropriate to consider values for k_a higher than 4, so it can be assumed that $1 \le k_a \le 4$. On the other hand, taking into account that the diffuse light is collected by the photodetector, it is necessary to consider values of $\widehat{\alpha_s}$ lower than α_s; that is to say, $0 \le k_s \le 1$. In any case, a value near 0 can be considered for k_s, according to previous experimental works [12].

It is clear that as long as α, k_a, and k_s are known for a tissue sample, its spectral coefficients α_a and α_s could be determined by

$$\alpha_s(\lambda) = \frac{1}{k_a - k_s}\left[k_a\alpha(\lambda) + \frac{1}{L}\ln[\widehat{T_t}(\lambda)]\right],$$
$$\alpha_a(\lambda) = \alpha(\lambda) - \alpha_s(\lambda), \tag{3}$$

which is easily deduced from Eqs. (1) and (2). However, the actual procedure is not so easy. Although α is measured using the method based on fiber collimators [18], the values of k_a and k_s cannot be determined, but can only be delimited between the maximum and minimum values. By means of Eq. (3) and taking into account that $\alpha_a \ge 0$, we can delimit the interval $0 \le k_s \le \hat{\alpha}/\alpha \ll 1$, which is in agreement with Shi *et al.* [12]. In addition, taking derivatives of Eq. (3) with respect to k_a and k_s · it can be seen that α_s is an increasing function of k_a and k_s, since $k_a > k_s$ (and, therefore, α_a is a decreasing function of k_a and k_s). Thus, to determine maximum and minimum values of α_a and α_s, it is only necessary to consider extreme values of the pair (k_a, k_s); in other words, $(k_a = 1, k_s = 0)$ and $(k_a = 4, k_s = \hat{\alpha}/\alpha)$. By measuring several samples of different thickness, it can be verified that the values of α_a and α_s are compatible with all the samples and more precise limits can be established for both magnitudes.

3. RESULTS AND DISCUSSION

The transmittances of three brain samples with thicknesses of 25 μm, 50 μm, and 100 μm, respectively, were measured by means of both systems. In Fig. 2, α and $\hat{\alpha}$ are gathered as a function of the wavelength. As the scattered light is avoided, the attenuation coefficient measured by means of fiber collimators is always higher that the effective attenuation coefficient measured by means of the spectrophotometer. By using a spectrophotometer, $\hat{\alpha}$ changes with the sample thickness, due probably to different k_a values. By applying the procedure described previously, the maximum and minimum allowed values of α_a are determined for the three brain samples. As can be seen in Fig. 3, compatible values for the three thicknesses fall between the maximum values (obtained for 100 μm of the sample length) and minimum values (obtained for 25 μm of the sample length). Using the spectrophotometer, significant variations among tissues were revealed, reflecting the high variability of the samples and the dependency on thickness, measured area, and water content [8,12].

Taking into account our theoretical frame, the α_a coefficient can be determined as the mean value of its maximum and minimum allowed values and, at the same time, the error can be estimated, taking into account both extreme values. Then, α_s is computed as the difference between the α and α_a coefficients. Finally, it is necessary to check that the spectrum of the α_a is not senseless. If this spectrum is correct, it should be reproduced by fitting of k_a and k_s for each of the three samples. The mean and the extreme values of α_a and α_s coefficients are shown in Figs. 4 and 5, respectively. The α_s coefficient is affected by an average relative error of 5%, although it varies from 3% up to 12% along the measured spectrum. On the other hand, the α_a coefficient has an average relative error around 37%, with variations between 22% and 45%. Nevertheless, the same error on α_a and α_s coefficients would be obtained by an increment of 0.11 in transmittance, which is a usual variation between measurements made in different points of a sample.

Measured biological samples with high α_a and a relatively small light scattering have been previously described. Similar

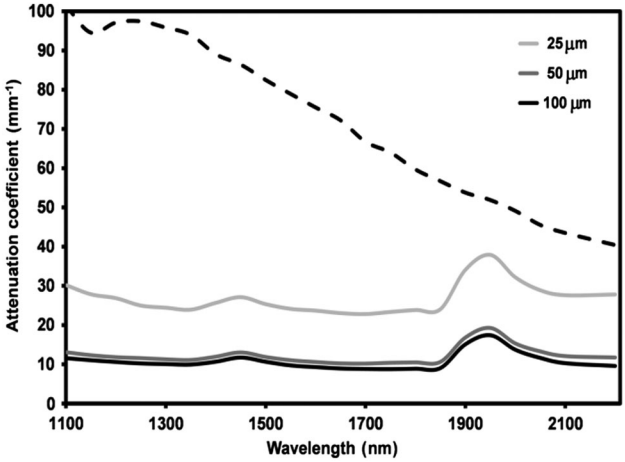

Fig. 2. Attenuation coefficient $\alpha(\lambda)$ of brain tissue measured by fiber collimators (dashed line) and effective attenuation coefficient $\hat{\alpha}(\lambda)$ by spectrophotometer (solid lines). The coefficient obtained by the first method is always higher because the scattered light is avoided.

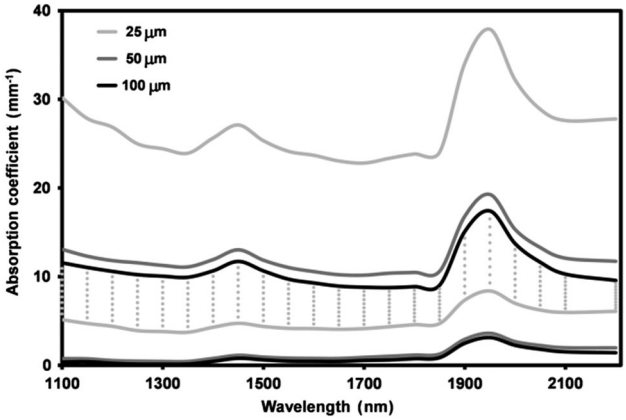

Fig. 3. Maximum and minimum allowed values of the absorption coefficient obtained for the three brain samples. Actual compatible values fall between maximum values for a 100 μm sample and minimum values for a 25 μm sample (dotted region).

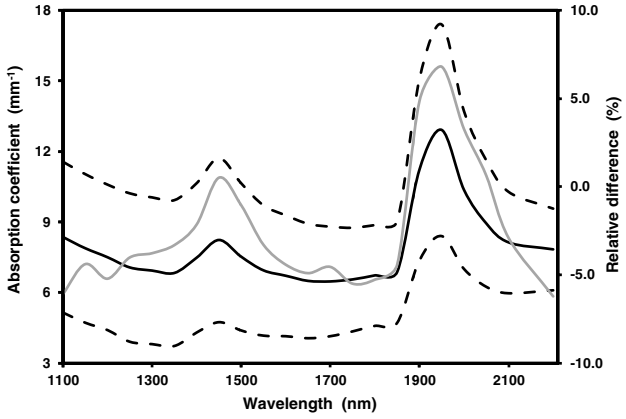

Fig. 4. Spectral absorption coefficient of the brain tissue: mean values (solid black line) and maximum/minimum values (dashed black lines). The relative difference of the fitted spectrum for the sample of 100 μm regarding the mean values is plotted in a solid gray line.

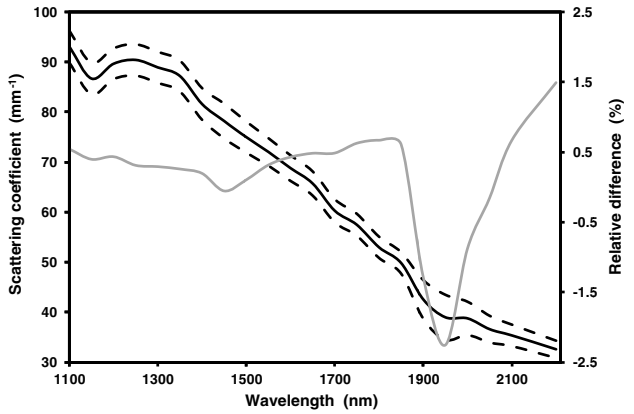

Fig. 5. Spectral scattering coefficient of the brain tissue: mean values (solid black line) and maximum/minimum values (dashed black lines). The relative difference of the fitted spectrum for the sample of 100 μm regarding the mean values is plotted in solid gray line.

results to those herein described were found in the α_a coefficient, although the α_s coefficient was usually estimated with the power-law decay function $\alpha_s \sim \lambda^{-b}$, with $1 < b < 2$ for most biological tissues [4,16]. Considering the measurements for the studied tissues at 1450 and 1950 nm, we can observe that the absorbance in these regions was higher than the absorbance in other zones, where it remains constant. These wavelengths correspond to the absorption of water, indicating the high water content in the studied samples [4,12,16]. Due to the composition of the same structural elements with different percentages, some weak additional absorption peaks were found, depending on the different type of biological sample (such as a cow or pig) were described [16]. For tissues, most of the weak bands of lipids, collagen, and proteins overlapped with the stronger water bands. The first overtone of O-H stretching has a peak at 1450 nm, and a second contribution can be found combined at 1930 nm and at 1975 nm. In the absorption spectra, mainly primary peaks from the lipids (1200 nm, first overtone of C-H stretching at 1730 nm and 1750 nm), from the proteins (first overtone of N-H stretching around 1420 nm to 1600 nm), and from the collagen (1200 nm and 1725 nm) can be weakly distinguished. The low differences until 1300 nm could be explained by the superposition of the absorption of water, lipids, and collagen from the different tissues or cholesterol.

As we have mentioned, we checked that the results reached by means of this procedure were not senseless, and we confirmed that absorption and scattering coefficients can be properly reproduced by fitting k_a and k_s values for the three tissue samples (see Figs. 4 and 5). In fact, with $k_a = 3.17$ and $k_s = 0.021$ for the 25 μm length sample, with $k_a = 1.40$ and $k_s = 0.018$ for the 50 μm length sample, and with $k_a = 1.27$ and $k_s = 0.023$ for the 100 μm length sample, α_a and α_s spectra are reproduced with a mean relative error of 5% and 1%, respectively. As was expected, k_s only changes slightly since it mainly obeys a geometrical relationship between the area of the photodetector and the scattering angle, which is not altered between samples due to their low thickness.

This experimental procedure was also applied to retina tissues. The mean and the extreme values of α_a and α_s coefficients are shown in Figs. 6 and 7, respectively. Parameter α_s is affected by a mean relative error of 1%, although it varies from 0.8% up to 2% along its spectrum. However, the α_a coefficient has a mean relative error around 24%, with variations between 16% and 37%. The absorption and scattering coefficients are also reproduced (see Figs. 6 and 7), with $k_a = 2.70$ and $k_s = 0.0050$ for the 25 μm length sample, with $k_a = 3.00$ and $k_s = 0.034$ for the 50 μm length sample and with $k_a = 1.12$ and $k_s = 0.0047$ for the 100 μm length sample.

Finally, the spectral coefficients α_a and α_s for different biological tissues (heart, brain, spleen, retina, and kidney) were determined by applying the described experimental procedure. The results are shown in Figs. 8 and 9. The α_a coefficient has a similar behavior for all the studied tissues, with two clearly visible peaks (at 1450 nm and 1930 nm) that are due to water absorption. Therefore, we can differentiate two spectral windows with low absorption: from 1150 nm to 1400 nm and from 1550 nm to 1850 nm. However, α_s coefficients only have slight spectral variations, and they are always much greater than α_a

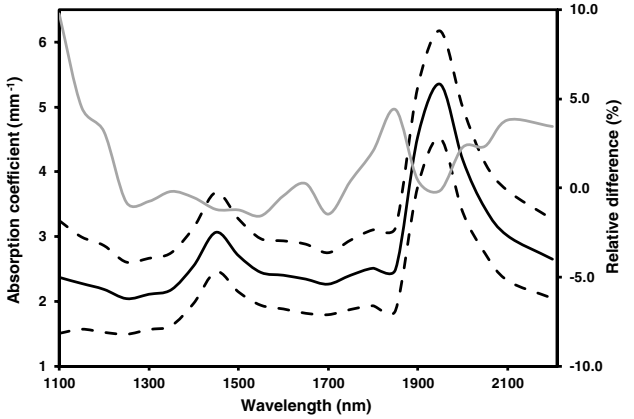

Fig. 6. Spectral absorption coefficient of the retina tissue: mean values (solid black line) and maximum/minimum values (dashed black lines). The relative difference of the fitted spectrum for the sample of 100 μm regarding the mean values is plotted in solid gray line.

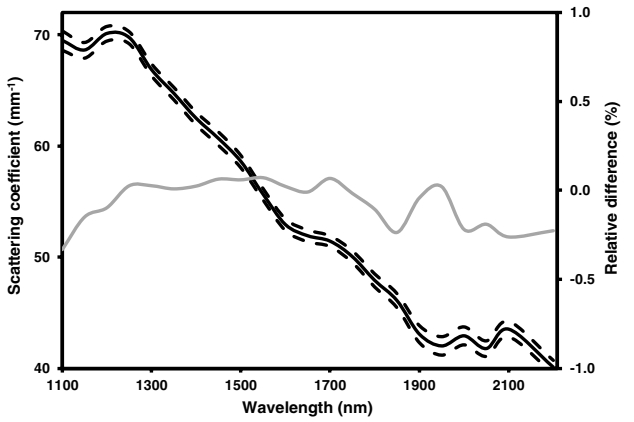

Fig. 7. Spectral scattering coefficient of the retina tissue: mean values (solid black line) and maximum/minimum values (dashed black lines). The relative difference of the fitted spectrum for the sample of 100 μm regarding the mean values is plotted in solid gray line.

values. Therefore, α coefficients decrease with the size of the wavelength, and longer wavelengths should be preferred to obtain higher penetration depths. This behavior is due mainly to the scattering coefficient, which is one order of magnitude higher than the absorption coefficient. In particular, the scattering coefficient is $\sim 50\%$ lower at 2100 nm compared to 1100 nm in the heart, spleen, brain, and kidney, in spite of the higher absorption.

Strong differences are found in the values of the absorption and the scattering coefficients reported by several authors. These differences are due to the different methods employed to measure the attenuation coefficient. In our case, we measured it by eliminating all the scattered light; in other words, by detecting only the ballistic photons. Consequently, the values obtained for the attenuation coefficient are very high compared to the values obtained by other authors. Some authors measured the attenuation coefficient without removing all the scattered light and therefore reported values significantly lower than our values

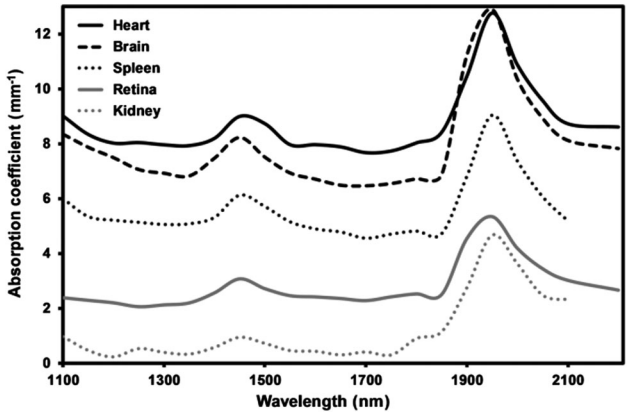

Fig. 8. Spectral absorption coefficient for several biological tissues.

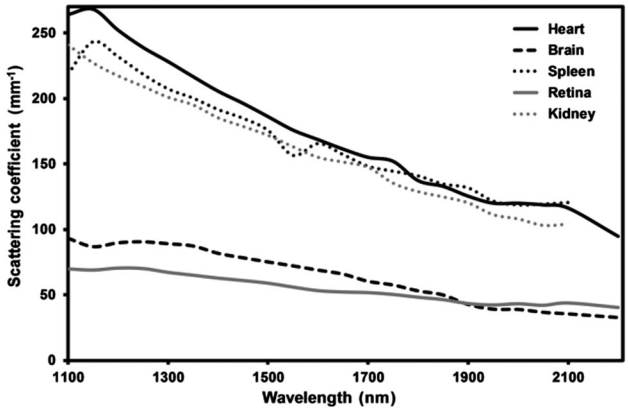

Fig. 9. Spectral scattering coefficient for several biological tissues.

[10,16,24]. For example, in [10] the authors show an attenuation coefficient of 1 mm^{-1} at 1700 nm (which means that the transmission factor of tissues of 1 mm thickness is as high as 37%) for brain tissue, whereas our attenuation coefficient is around 70 mm^{-1}. D'Esposito *et al.* [5] also reported very low values (between 0.5 mm^{-1} and 1.5 mm^{-1}) using optically cleared tissues. In fact, [5] includes an enlightening photograph, which shows how the chemical clearing transforms opaque tissues into almost transparent tissues. Nevertheless, the profiles of the absorption spectra are similar. However, other authors report intermediate values compared to these values since they partially suppress the scattered light [4,19,29,30]. Thus, they have reported transmittance values (around 10^{-4} for a sample of 1 mm length) that are compatible with an attenuation coefficient around 10 mm^{-1} at 1700 nm. Logically, they are effective values useful for each author since the eliminated quantity of scattered light depends on the technique used (optical coherence tomography, for example) and on the properties of the measured sample (chemical constituents, delay between excision and measurement, fixation, and water content, for example).

Different theoretical models can be found in the bibliography that are based on different experimental attenuation coefficients and assumptions. In the present work, what we believe is a different method to determine the absorption and the scattering coefficients has been presented, based only on measurements of

attenuation in two experimental setups. It is necessary to take into account that biological tissues present a high complexity, while most of soft tissues are close to optically soft media in the therapeutic window [7–14]. In other words, the absorption coefficient and the transport scattering coefficient are practically independent of each other. The absorption coefficient of a tissue is determined by the local value of spectral absorption index of the substances and is totally insensitive to the tissue morphology. On the contrary, the transport scattering coefficient is practically independent of the absorption and determined mainly by the tissue morphology, which is responsible for the spatial variation of the refraction index. Although scattering spectra could be computed using the traditional theoretical expression $\mu_s = \alpha\lambda^{-\omega} + b\lambda^{-4}$ (Mie and Rayleigh approximations), it would be a clear contradiction with the point of view of our method, which determines absorption and scattering spectra by only experimental measurements to provide a more realistic description of the biological tissues. A limitation of our results is the assumption of the nonwave-dependence of the k_a and k_s coefficients. Future works in this field should consider this assumption to obtain more specific knowledge of the optical properties of biological tissues.

4. CONCLUSION

In conclusion, we have presented two complementary techniques for the experimental measurement of the attenuation coefficient, both scattering and absorption, of biological tissues. We believe we have demonstrated the viability of our method since it is fully compatible with our measurements, and it has been satisfactorily applied to samples of different biological tissues. Thus, this method could be applied to measurements with different kinds of tissues or with samples prepared in a different way.

Funding. Ministerio de Economía, Industria y Competitividad, Gobierno de España (FIS2013-44174-P); Instituto de Salud Carlos III (RD16/0008/0016); Gobierno de Aragón (B08_17R, T20_17R); Universidad de Zaragoza (UZ-SANTANDER); Instituto Aragonés de Ciencias de la Salud (C060/2014).

Disclosures. The authors declare no conflicts of interest.

REFERENCES

1. D. Kobat, M. E. Durst, N. Nishimura, A. W. Wong, C. B. Schaffer, and C. Xu, "Deep tissue multiphoton microscopy using longer wavelength excitation," Opt. Express **17**, 13354–13364 (2009).
2. D. Kobat, N. G. Horton, and C. Xu, "In vivo two-photon microscopy to 1.6-mm depth in mouse cortex," J. Biomed. Opt. **16**, 106014 (2011).
3. R. K. Wang and L. An, "Doppler optical micro-angiography for volumetric imaging of vascular perfusion in vivo," Opt. Express **17**, 8926–8940 (2009).
4. S. P. Chong, C. W. Merkle, D. F. Cooke, T. Zhang, H. Radhakrishnan, L. Krubitzer, and V. J. Srinivasan, "Noninvasive, in vivo imaging of subcortical mouse brain regions with 1.7 μm optical coherence tomography," Opt. Lett. **40**, 4911–4944 (2015).
5. A. D'Esposito, D. Nikitichev, A. Desjardins, S. Walker-Samuel, and M. F. Lythgoe, "Quantification of light attenuation in optically cleared mouse brains," J. Biomed. Opt. **20**, 80503 (2015).
6. N. Bosschaart, G. J. Edelman, M. C. Aalders, T. G. van Leeuwen, and D. J. Faber, "A literature review and novel theoretical approach on the optical properties of whole blood," Laser Med. Sci. **29**, 453–479 (2014).
7. B. C. Wilson and S. L. Jacques, "Optical reflectance and transmittance of tissues: principles and applications," IEEE J. Quantum Electron. **26**, 2186–2199 (1990).
8. S. L. Jacques, "Optical properties of biological tissues: a review," Phys. Med. Biol. **58**, R37–R61 (2013).
9. A. N. Bashkatov, E. A. Genina, and V. V. Tuchin, "Optical properties of skin, subcutaneous, and muscle tissues: a review," J. Innov. Opt. Health Sci. **4**, 9 (2011).
10. S. Golovynskyi, I. Golovynska, L. I. Stepanova, O. I. Datsenko, L. Liu, J. Qu, and T. Y. Ohulchanskyy, "Optical windows for head tissues in near-infrared and short-wave infrared regions: approaching transcranial light applications," J. Biophoton. **11**, e201800141 (2018).
11. D. C. Sordillo, L. A. Sordillo, P. P. Sordillo, L. Shi, and R. R. Alfano, "Short wavelength infrared optical windows for evaluation of benign and malignant tissues," J. Biomed. Opt. **22**, 45002 (2017).
12. L. Shi, L. A. Sordillo, A. Rodriguez-Contreras, and R. R. Alfano, "Transmission in near-infrared optical windows for deep brain imaging," J. Biophoton. **9**, 38–43 (2016).
13. A. M. Smith, M. C. Mancini, and S. Nie, "Bioimaging: second window for in vivo imaging," Nat. Nanotechnol **4**, 710–711 (2009).
14. R. R. Anderson and J. A. Parrish, in *Optical Properties of Human Skin (The Science of Photomedicine)*, J. D. Regan and J. A. Parrish, eds. (Springer, 1982), pp. 147.
15. A. N. Bashkatov, E. A. Genina, V. I. Kochubey, and V. V. Tuchin, "Optical properties of human skin, subcutaneous and mucous tissues in the wavelength range from 400 to 2000 nm," J. Phys. D **38**, 2543–2555 (2005).
16. S. A. Filatova, I. A. Shcherbakov, and V. B. Tsvetkov, "Optical properties of animal tissues in the wavelength range from 350 to 2600 nm," J. Biomed. Opt. **22**, 035009 (2017).
17. C. Fornaini, M. Sozzi, E. Merigo, P. Pasotti, S. Selleri, and A. Cucinotta, "Supercontinuum source in the investigation of laser-tissue interactions: 'ex vivo study'," J. Biomed. **2**, 12 (2017).
18. J. E. Saldaña-Díaz, S. Jarabo, F. J. Salgado-Remacha, L. Perdices, I. Pinilla, and A. Sánchez-Cano, "Spectral attenuation of brain and retina tissues in the near-infrared range measured using a fiber-based supercontinuum device," J. Biophoton. **10**, 1105–1109 (2017).
19. H. Kawagoe, S. Ishida, M. Aramaki, Y. Sakakibara, E. Omoda, H. Kataura, and N. Nishizawa, "Development of a high power supercontinuum source in the 1.7 μm wavelength region for highly penetrative ultrahigh-resolution optical coherence tomography," Biomed. Opt. Express **5**, 932–943 (2014).
20. M. Wang, C. Wu, D. Sinefeld, B. Li, F. Xia, and C. Xu, "Comparing the effective attenuation lengths for long wavelength in vivo imaging of the mouse brain," Biomed. Opt. Express **9**, 3534–3543 (2018).
21. L. X. Ma, B. W. Xie, C. C. Wang, and L. H. Liu, "Radiative transfer in dispersed media: Considering the effect of host medium absorption on particle scattering," J. Quant. Spectrosc. Radiat. Transf. **230**, 24–35 (2019).
22. L. A. Dombrovsky, "A new method to retrieve spectral absorption coefficient of highly-scattering and weakly-absorbing materials," J. Quant. Spectrosc. Radiat. Transf. **172**, 75–82 (2016).
23. L. Dombrovsky, K. Ganesan, and W. Lipinski, "Combined two-flux approximation and Monte Carlo model for identification of radiative properties of highly scattering dispersed materials," Comput. Therm. Sci. **4**, 365–378 (2012).
24. L. A. Sordillo, Y. Pu, S. Pratavieira, Y. Budansky, and R. R. Alfano, "Deep optical imaging of tissue using the second and third near-infrared spectral windows," J. Biomed. Opt. **19**, 056004 (2014).
25. L. A. Sordillo, L. Lindwasser, Y. Budansky, P. Leproux, and R. R. Alfano, "Near-infrared supercontinuum laser beam source in the second and third near-infrared optical windows used to image more deeply through thick tissue as compared with images from a lamp source," J. Biomed. Opt. **20**, 030501 (2015).
26. S. Andersson-Engels, R. Berg, S. Svanberg, and O. Jarlman, "Time-resolved transillumination for medical diagnostics," Opt. Lett. **15**, 1179–1181 (1990).

27. G. Mitic, J. Kölzer, J. Otto, E. Plies, G. Sölkner, and W. Zinth, "Time-gated transillumination of biological tissues and tissue like phantoms," Appl. Opt. **33**, 6699–6710 (1994).
28. M. R. Hee, J. A. Izatt, J. M. Jacobson, J. G. Fujimoto, and E. A. Swanson, "Femtosecond transillumination optical coherence tomography," Opt. Lett. **18**, 950–952 (1993).
29. N. Nishizawa, H. Kawagoe, M. Yamanaka, M. Matsushima, K. Mori, and T. Kawabe, "Wavelength dependence of ultrahigh-resolution optical coherence tomography using supercontinuum for biomedical imaging," IEEE J. Sel. Top. Quantum Electron. **25**, 7101115 (2019).
30. U. Sharma, E. W. Chang, and S. H. Yun, "Long-wavelength optical coherence tomography at 1.7 μm for enhanced imaging depth," Opt. Express **16**, 19712–19723 (2008).